



Supplement of

Distributed acoustic sensing as a tool for subsurface mapping and seismic event monitoring: a proof of concept

Nicola Piana Agostinetti et al.

Correspondence to: Nicola Piana Agostinetti (nicola.pianaagostinetti@unimib.it)

The copyright of individual parts of the supplement might differ from the article licence.

Contents:

Fig. S1 – P-wave velocity profile adopted for locating micro-earthquakes

Fig. S2 – Modified Wadati diagram for deriving a V_p/V_s ratio

Fig. S[3-6] – Sample locations of local earthquakes from inversion of DAS and nodal data.

Table S1 – List of analyzed earthquakes.

1. Velocity Models

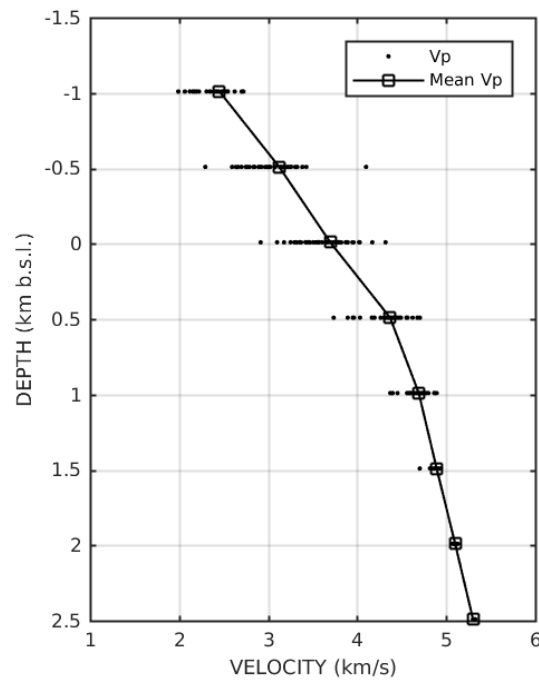


Fig. S1 – 1-D, P-wave velocity model derived from the 3D tomographic images of Singh and Foxall (2015), available at <https://gdr.openei.org/submissions/493> (University of Wisconsin, 2015). The velocity profile is derived by averaging velocities associated with nodes located along planes of constant depth.

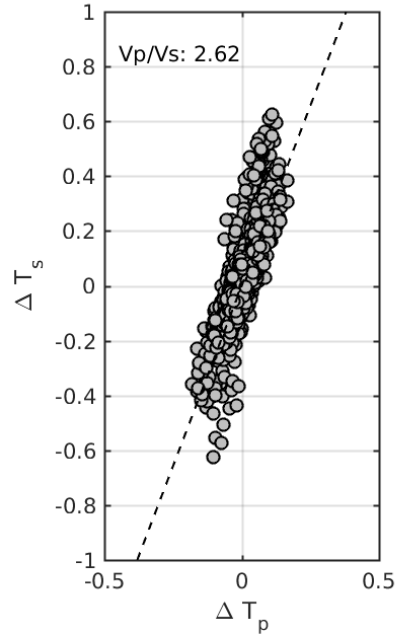


Fig. S2. Modified Wadati diagram applied to the differential P- and S-wave arrival times estimated at the nodal array for the 2016 March 14, 10:42:07 event. The estimated V_p / V_s ratio is equal to 2.6.

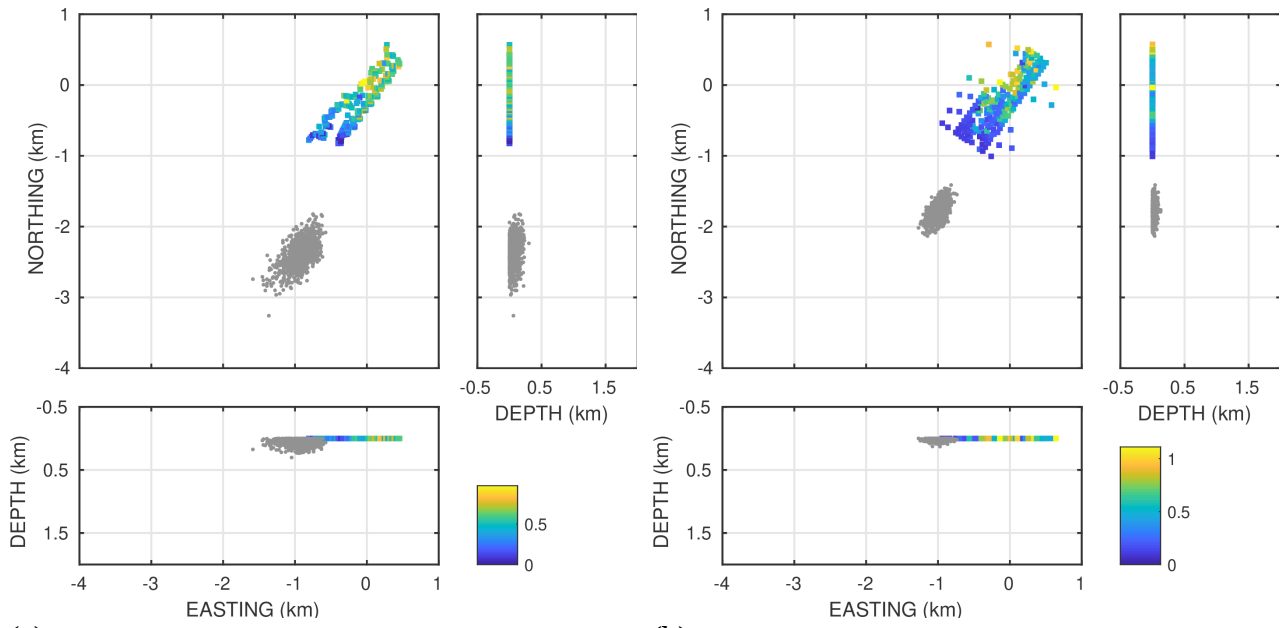
2. Local microseismicity

The comparison between locations obtained from automatically-picked DAS and nodal data is extended to four additional micro-earthquakes (Table S1). Two of these earthquakes (IDs 1 and 2) are from the NCEDC (2014) catalog, and were used as template events by Lin and Zhang (2018). The other two (IDs 3, 4) are from the list of matched-filter detections reported by these latter authors.

Table S1 – List of the analyzed earthquakes. Located events are taken from the NCEDC (2014) catalog.

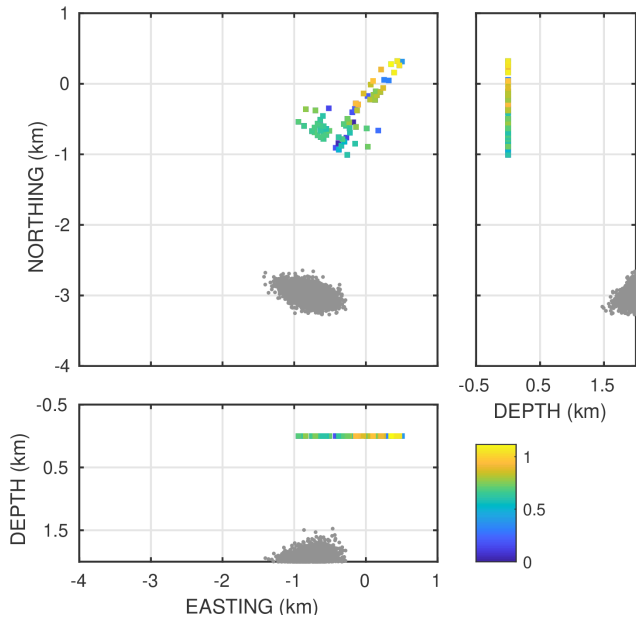
ID	date	time	ID NCEDC	Lat	Lon	Depth (km a.s.l.)	ML
1	2016-03-14	08:36:16.07	-	-	-	-	-
2	2016-03-14	08:37:10.54	-	-	-	-	-
3	2016-03-14	08:39:05.23	2201050	39.79350	-119.01717	-0.106	0.07
4	2016-03-14	12:11:34.92	2201051	39.79222	-119.01427	-0.424	-0.29

Event #1



(a)

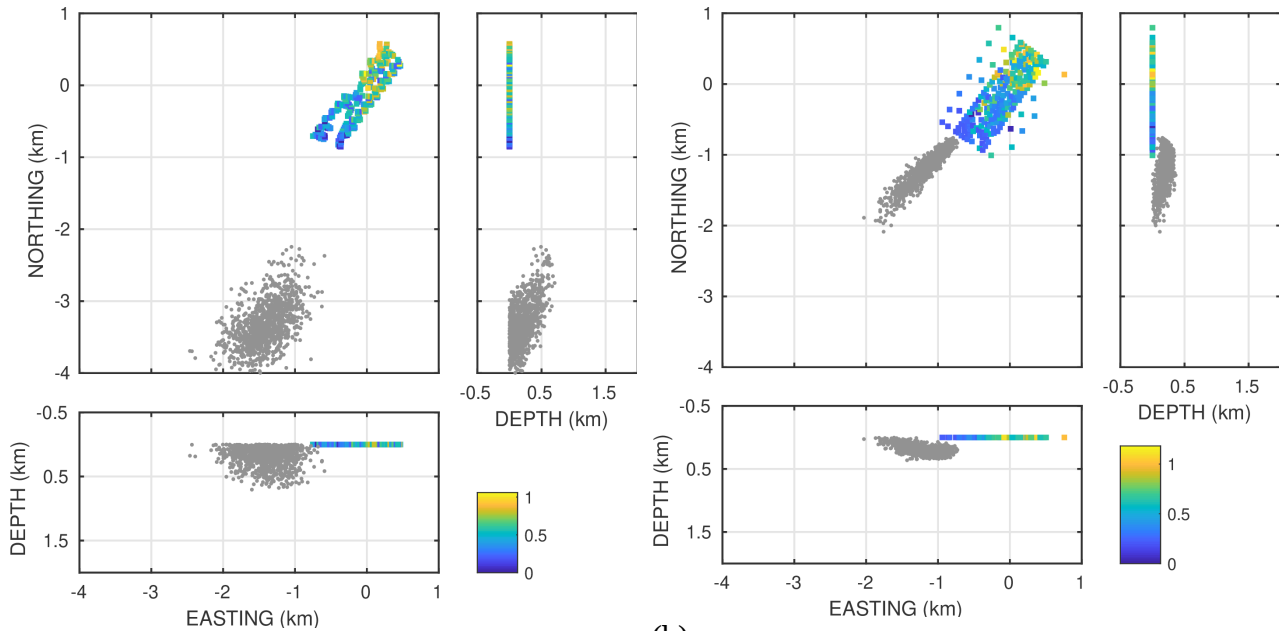
(b)



(c)

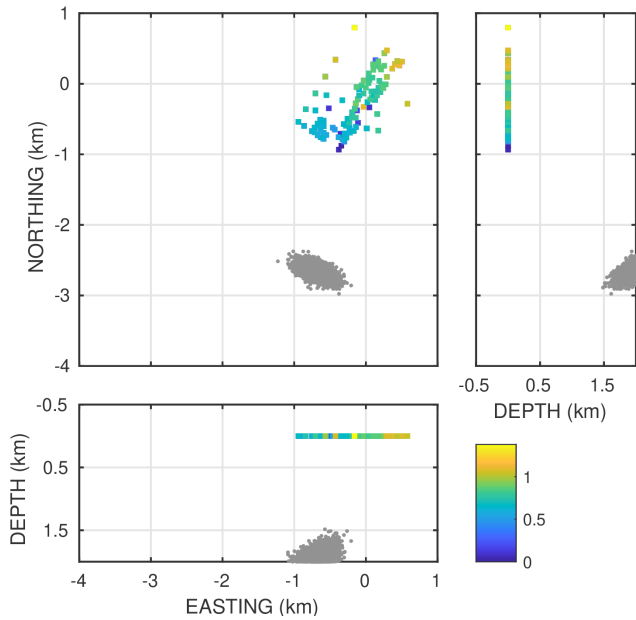
Fig. S3 – Location of event #2 in Table S1. (a) Samples of the likelihood function of source location (gray dots) derived from inversion of automatic picking of first onsets at the 239-elements DAS virtual array (colored squares). (b) The same as in (a), but for the vertical components of the nodal array. (c) Results from inversion of manual P- and S-wave time pickings at the nodal array. Inb all the panels, colors indicate the timing of picked P-wave arrivals, according to the color scale at the right.

Event #2



(a)

(b)



(c)

Fig. S4. The same as in Fig. S3, but for Event #4 in Table S1.

Event #3

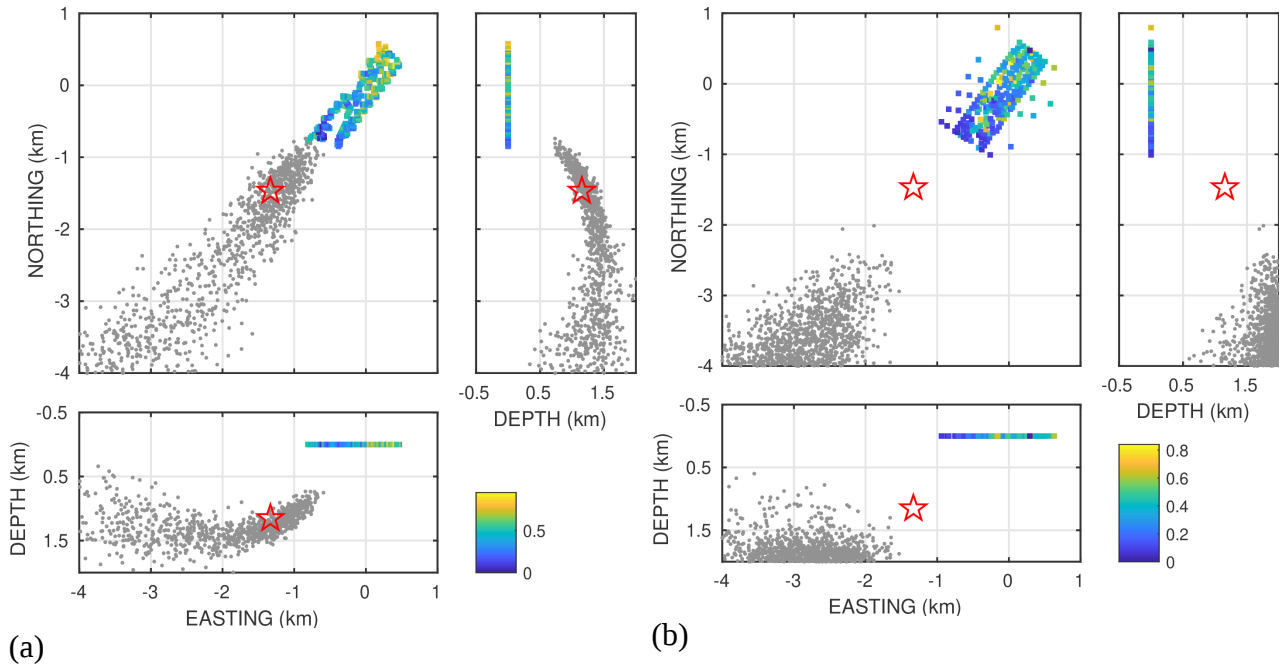


Fig. S5 – Location of event #5 in Table S1. (a) Samples of the likelihood function of source location (gray dots) derived from inversion of automatic picking of first onsets at the 239-elements DAS virtual array (colored squares). (b) The same as in (a), but for the vertical components of the nodal array. In both panels, colors indicate the timing of picked P-wave arrivals, according to the color scale at the right. The star indicate the reference location from the NCEDC (2014) catalog, also reported in Table S1.

Event #4

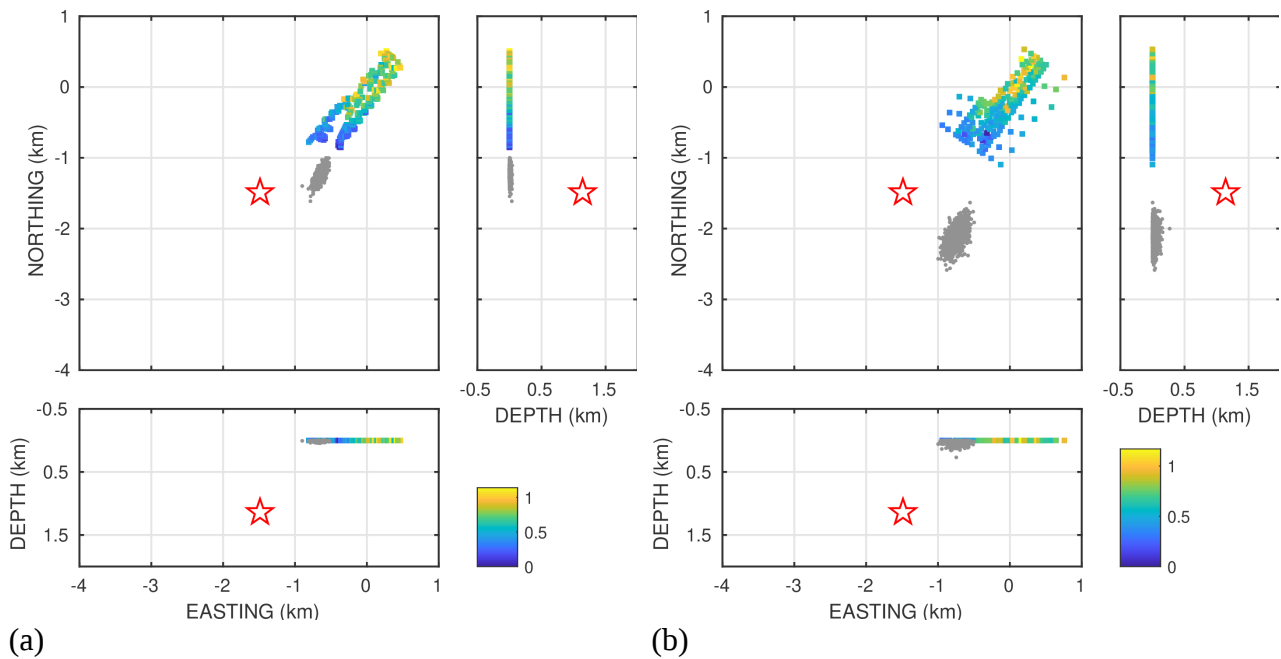


Fig. S6 – The same as in Fig. S5, but for event #8 in Table S1.

References

University of Wisconsin. (2015). *Bradys Geothermal Field MEQ Relocations 3D Velocity Models [data set]*. Retrieved from <https://dx.doi.org/10.15121/1196282>.

NCEDC (2014), Northern California Earthquake Data Center. UC Berkeley Seismological Laboratory. Dataset. doi:10.7932/NCEDC. Retrieved from <http://ncedc.org/egs/catalog-search.html> (last accessed December 1, 2021)